

# 1 A VTA GABAergic computational 2 model of dissociated reward 3 prediction error computation in 4 classical conditioning

5 **Pramod Kaushik<sup>1,3</sup>, Jérémie Naudé<sup>2</sup>, Surampudi Bapi Raju<sup>1</sup>, Frédéric  
6 Alexandre<sup>3,4,5\*</sup>**

\*For correspondence:

[frederic.alexandre@inria.fr](mailto:frederic.alexandre@inria.fr) (FA)

7 <sup>1</sup>International Institute of Information Technology, Hyderabad, India; <sup>2</sup>Neuroscience  
8 Paris-Seine, UPMC UMR 8246, Paris, France; <sup>3</sup>Inria Bordeaux Sud-Ouest, Talence, France;  
9 <sup>4</sup>LaBRI, University of Bordeaux, Bordeaux INP, CNRS, UMR 5800, Talence, France;  
10 <sup>5</sup>Institute of Neurodegenerative Diseases, University of Bordeaux, CNRS, UMR 5293,  
11 Bordeaux, France

---

13 **Abstract** Classical Conditioning is a fundamental learning mechanism where the Ventral  
14 Striatum is generally thought to be the source of inhibition to Ventral Tegmental Area (VTA)  
15 Dopamine neurons when a reward is expected. However, recent evidences point to a new  
16 candidate in VTA GABA encoding expectation for computing the reward prediction error in the VTA.  
17 In this system-level computational model, the VTA GABA signal is hypothesised to be a combination  
18 of magnitude and timing computed in the Peduncolopontine and Ventral Striatum respectively.  
19 This dissociation enables the model to explain recent results wherein Ventral Striatum lesions  
20 affected the temporal expectation of the reward but the magnitude of the reward was intact. This  
21 model also exhibits other features in classical conditioning namely, progressively decreasing firing  
22 for early rewards closer to the actual reward, twin peaks of VTA dopamine during training and  
23 cancellation of US dopamine after training.

---

## 25 Introduction

26  
27  
28 The phasic firing activity of midbrain dopamine neurons is believed to encode a reward prediction  
29 error, which can guide learning and serve as an incentive signal. In his famous experiment, Pavlov  
30 observed that if food follows the ring of a bell, a dog comes to salivate after the bell is rung.  
31 This process is called classical (or pavlovian) conditioning: an unconditioned response (salivation)  
32 originally associated with an *Unconditioned Stimulus* (US, the food) becomes conditionally elicited  
33 by a *Conditioned Stimulus* (CS, the bell ring). Schultz and collaborators examined the activity of  
34 midbrain dopamine neurons in primates, during a classical conditioning task similar to Pavlov's.  
35 They observed that originally, midbrain dopamine neurons responded with a burst of spikes to  
36 unexpected primary rewards (juice/water dripped in the mouth of thirsty primates), i.e. an US.  
37 After the primates learned the association between a tone CS and the reward US, dopamine cells  
38 responded to the reward-predicting CS. Moreover, these neurons stopped responding to US whose  
39 arrival was expected, being predicted by the CS. When cued rewards failed to be delivered, a large

40 percentage of dopamine neurons revealed a brief pause with respect to their background firing at  
41 the moment of expected reward in Figure 2.

This predictive behavior of VTA Dopamine neurons was linked to the *Temporal Difference Learning* algorithm in Reinforcement Learning (**Sutton and Barto, 1998**). The TD algorithm predicts a future reward that occurs at a specific state ahead of time after a given number of trials. This prediction is arrived through the computation of a reward prediction error (RPE) that enables learning the value of each state. It is represented by the equation:

$$\delta_t = r_t + \gamma \bar{V}_{t+1} - \bar{V}_t \quad (1)$$

42 where  $r_t$  is the reward (return) on time step  $t$ . Let  $\bar{V}_t$  be the correct prediction that is equal to the  
43 discounted sum of all future rewards. The discounting is done by powers of factor of  $\gamma$  such that  
44 reward at distant time step is less important as compared to recent rewards.

45 The TD algorithm is powerful in its heuristic value, as it links the activation of dopamine cells  
46 with classical conditioning. However, some properties of TD models are inconsistent with the  
47 electrophysiological data, and it lacks the biological realism needed to explain the mechanisms  
48 through which RPE-like activity emerges in dopamine cells. Most inconsistencies are concerned with  
49 the way time is represented in the TD model. Whereas the TD error signal travels back in time from  
50 US to CS when learning progresses, it has been reported in (**Schultz et al., 1997**) that US-related  
51 activation of VTA slowly decreases while the CS-related one increases. Ramping dopamine activity  
52 during the CS-US interval has been proposed to reflect back-propagating error signals averaged  
53 over trials (**Niv et al., 2005**) but this ramping can be observed in individual trials and is actually  
54 related to reward uncertainty (**Fiorillo et al., 2003**)(**Fiorillo et al., 2005**). More importantly, when  
55 US is delivered earlier than predicted, VTA dopaminergic neurons are activated at the actual time  
56 of the US but not at the usual time of reward (**Hollerman and Schultz, 1998**), contrarily to what is  
57 predicted by TD. Critically, when striatum is lesioned, experiments (**Takahashi et al., 2016**) show  
58 that VTA dopaminergic neurons signal a RPE when reward magnitude changes, but not when time  
59 of the reward is modified. This suggests that learning about reward timing is computationally  
60 and anatomically separated from learning about reward magnitude, i.e. a completely different  
61 implementation of reinforcement learning than is usually considered (**Joel et al., 2002**).

62 Here we sought a system-level account of how the CS-US interval duration and the value of  
63 the reward are separately learned, and how these two features are combined to give rise to  
64 dopaminergic phasic activity. In particular, we considered two components of the meso-limbic  
65 loops that have been overlooked in previous models: VTA GABA cells and neurons from the  
66 Pedunculopontine Nucleus (PPN). We propose that VTA GABA neurons provide inhibitory drive  
67 onto VTA DA neurons (**Eshel et al., 2015**), display persistent firing during the CS-US interval (**Cohen**  
68 **et al., 2012**) and are necessary to compute the RPE in DA cells (**Eshel et al., 2015**). Neurons from  
69 the PPN project to both VTA DA and GABA neurons and have been found necessary for appetitive  
70 conditioning (**Yau et al., 2016**). PPN neurons are classically believed to signal the delivery of  
71 actual reward (**Vitay and Hamker, 2014**). However, during conditioning, two types of response  
72 are recorded from neurons from the PPN: neurons responding to the actual reward magnitude,  
73 and a persistent neuronal firing during the CS-US interval, reflecting the prediction or expected  
74 reward magnitude (**Okada and Kobayashi, 2009**)(**Okada and Kobayashi, 2013**). Here we show that  
75 a system-level computational model can account for these yet-unexplained physiological and lesion  
76 data. We propose that the Ventral Striatum learns the reward timing and the Amygdala the reward  
77 magnitude, which is then transferred to the PPN. Expected reward timing and magnitude are  
78 subsequently combined at the level of VTA GABA cells to compute the expectation term needed by  
79 VTA DA neurons to generate a prediction error. We furthermore provide testable predictions for  
80 future experiments, on the role of PPN and VTA GABA in classical conditioning.

## 81 Results

82

83 We built a system-level network in which reward prediction error (RPE) emerges during learning,  
84 from the interaction of the neuronal ensembles representing RPE computation. To illustrate how  
85 RPE is computed in the network, we subjected it to in silico experimental scenarios similar to a  
86 conditioning task. This analogue of classical conditioning consists in the repeated pairing of a CS  
87 with the US, separated by a fixed interval duration. The in silico experiments below examine how the  
88 value (magnitude) of the US reward and the duration of the CS-US interval are learned separately,  
89 and combined by VTA GABA cells. In turn, VTA GABA neurons provide the expectation term used to  
90 cancel the excitation of dopamine cells by the US, at the time of the expected reward (*Cohen et al.,*  
91 *2012*)(*Eshel et al., 2015*). Finally, we show how this new model provides a better description of  
92 experimental data that have been left unexplained yet, i.e. how dopamine cells respond to rewards  
93 delivered earlier than expected (*Fiorillo et al., 2008*), and how value and timing are dissociated by  
94 VS lesions (*Takahashi et al., 2016*).

## 95 Model Architecture

96 The system-level computational model attempts to explain how the dopamine reward prediction  
97 error is computed in appetitive conditioning in the VTA through understanding the roles of VTA GABA  
98 and Peduncolopontine (PPN) neurons. The model is shown in Figure 1. The model focuses on the  
99 computation inside the VTA carried out by two populations viz., the VTA DA and VTA GABA neurons.  
100 Lateral Hypothalamus (LH) projects to PPN RD and VS and these in turn project to VTA DA and  
101 VTA GABA respectively. When reward is delivered, it is reported to fire the Lateral Hypothalamus  
102 (LH) and activates the LH → PPN RD (Reward delivery) → VTA Dopamine pathway resulting in  
103 US dopamine firing prior to any sort of learning (*Semba and Fibiger, 1992; Lokwan et al., 1999*).  
104 Basolateral Amygdala (BLA) learns the magnitude of the US through the projections from VTA  
105 DA to BLA, which signal a reward prediction error that modulates synaptic plasticity. A pathway  
106 from LH to BLA learns that BLA firing for CS has the same amplitude as the US-induced firing  
107 (*Sah et al., 2003*). The immediate firing in response to the CS occurs through the BLA recognizing  
108 the cue encoded by the Infero-temporal cortex (IT), with BLA activating the VTA DA through the  
109 BLA → CE → PPN RD → VTA DA pathway. The Central Nucleus of the Amygdala (CE) has excitatory  
110 projections on PPN FT (Fixation Target) (*Okada and Kobayashi, 2013*) (*Kobayashi and Okada, 2007*)  
111 which displays persistent activity unless strongly inhibited. The LH also projects to the VS, which  
112 is also modulated by VTA DA neurons. Finally, excitatory projections from PPN FT and inhibitory  
113 projections from VS neurons to VTA GABA enable the final reward cancellation of VTA DA observed  
114 in electro-physiological experiments.

## 115 Control Scenario

116 In the following, we show how a reward prediction error emerges in VTA Dopamine cells with  
117 learning, as a consequence of network dynamics and plasticity.

### 118 • Initial Trial

119 The arrival of an unexpected reward induces a firing in the LH neurons. This LH firing  
120 subsequently activates VTA Dopamine neurons, through the PPN RD neurons (Figure 3 B top  
121 panel Trial1, Figure 3 C top panel Trial 1). Hence, the model reproduces that VTA Dopamine  
122 neurons fire upon the delivery of an unexpected reward. No activity in BLA and Ventral  
123 Striatum (VS) and VTA GABA (Figure 3 B bottom panel Trial1) is observed at this stage of  
124 learning. Indeed, Basolateral Amygdala (BLA) has not yet learned to associate the magnitude  
125 of the CS with the US, and the Ventral Striatum (VS) the timing of the CS-US interval duration.  
126 Hence, there is no expectation at the arrival of the CS.

### 127 • Partial Conditioning

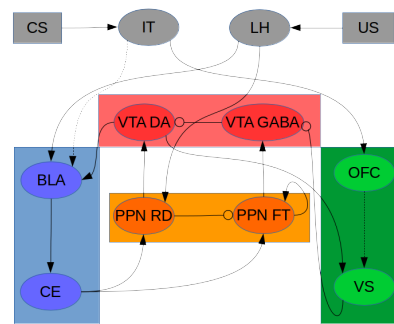


**Figure 1.** Model diagram illustrating the neuronal structures and their connections involved in Reward Prediction Error (RPE) computation. Pointed arrows represent excitatory connections, while rounded arrows represent inhibitory projections. Dashed lines represent learnable connections, while solid lines represent fixed connections in the model. Ventral Tegmental Area has Dopamine (DA) and GABA populations which play a central role in computing RPE. This RPE is transmitted to Basolateral Amygdala (BLA) and the Ventral Striatum (VS) where the modulatory connections undergo change depending on this signal. Both the VTA structures receive inputs from distinct Pedunculo-pontine (PPN) neural populations. The PPN Reward Delivery (RD) neurons deliver reward to VTA DA neurons from the Lateral Hypothalamus (LH) which receives the unconditioned stimulus (US). The PPN Fixation target (FT) neurons receive their projections from the Central Nucleus (CE) of the Amygdala and these PPN neurons along with Ventral Striatum (VS) project to VTA GABA forming the inhibitory signal that cancels the VTA DA upon reward delivery. The BLA is regarded to learn the association between unconditioned stimulus (US) and the conditioned stimulus (CS) and produces the anticipatory firing in VTA DA through the BLA->CE->PPN RD->VTA DA pathway. The VS is posited to learn the timing of the interval and it has inhibitory projections on VTA GABA.

128 The synaptic weights between IT and BLA are updated after each rewarding trial. Consequently,  
 129 after a few trials (7 in our simulations), the BLA starts responding to the CS stimulus. This  
 130 progressive learning in the BLA generates firing in VTA DA (Figure 3 B top panel) through  
 131 PPN RD (Figure 3 C top panel) in response to the arrival of the CS, corresponding to a partial  
 132 prediction of reward. BLA activity also generates a partial expectation through tonic firing  
 133 in PPN FT (Figure 3 C bottom panel Trial 7). Hence, a partial cancellation of VTA dopamine  
 134 neurons happens at this stage. At this stage, the time interval has been completely learned,  
 135 contrary to the learning of the US magnitude.

136 This corresponds to the activity of the Ventral Striatum reaching its minimum at the exact  
 137 moment of reward. Hence, the VS does not exert any inhibition at the end of the interval,  
 138 which results in the inhibition of VTA DA neurons at the expected time of the US. However,  
 139 as the US magnitude is not fully learned yet, the activity of PPN FT to VTA GABA pathway  
 140 only results in partial cancellation of VTA DA activity upon US delivery. This is consistent  
 141 with experimental results on Partial conditioning (*Pan et al., 2005*), and designed as a partial  
 142 expectation in the TD framework. (Figure 3 B bottom panel Trial 7). This partial expectation  
 143 consists in a twin peak of VTA firing, at the respective times of the CS and the US.

144 • Complete Reward Cancellation

145 The final state of the circuit, after 16 CS-US pairings, is given in Figure 3 A. The magnitude of  
 146 expectation originates from the CS firing in the Central Amygdala (CE) and is maintained in the  
 147 PPN FT through a self-sustaining mechanism (*Okada and Kobayashi, 2013*) (*Kobayashi and  
 148 Okada, 2007*). At the end of learning, the BLA neurons have reached an asymptote in their  
 149 firing, which encodes for reward magnitude. Hence, PPN FT neurons display maximum tonic  
 150 activity after the presentation of the CS. In parallel, as in partial conditioning, the presentation  
 151 of the CS, which fires the IT and thereby the Orbitofrontal Cortex (OFC) (*Carmichael and Price,  
 152 1995*), activates the VS that encodes the interval timing. It acts similar to a negative integrator

153 and progressively lowers the inhibition that VS exerts on PPN FT, to reach zero inhibition at  
154 the expected time of the reward. Both signals are combined by VTA GABA, the activity of which  
155 peaks at the time of the reward (Figure 3 B bottom panel Trial 16), cancelling VTA dopamine,  
156 which no longer shows firing at the time of the US when reward arrives through the LH (Figure  
157 3 B top panel Trial 16).

158 The magnitude of expectation originates from the CS firing in the Central Amygdala (CE)  
159 and maintained in the PPN FT through a self-sustaining mechanism (*Okada and Kobayashi,*  
160 *2013*) (*Kobayashi and Okada, 2007*). The GABA firing in the VTA is reflective of this (*Yau et al.,*  
161 *2016*) and the PPN FT integrates the magnitude from the Central Amygdala (CE) and timing  
162 information from the VS to achieve the ramping signal that encodes both time and magnitude  
163 of the reward delivery.

## 164 **Variability in Magnitude and Time**

### 165 1. Variability in Timing

166 When a reward is delivered earlier than expected (i.e. with a shorter delay than the CS-US  
167 interval that has been learned), US firing is observed in VTA dopamine neurons. More precisely,  
168 in this case of earlier-than-expected US reward, VTA dopamine neurons fire less than the  
169 initial (before learning) firing observed at US delivery. This is consistent with the US being  
170 expected, albeit not at this precise timing. An interpretation would be that partial expectations  
171 are generated during the CS-US interval, hence the reward prediction decreases with time  
172 until the expected timing of US delivery. In our model, we observed that the earlier the  
173 reward was delivered, the higher was the VTA DA firing (Figure 4 B). VTA DA firing in Figure 4  
174 A (middle left panel) shows a reward delivered before the half-way-point (at the 100<sup>th</sup> time  
175 step) evoking a dopamine firing, but less than the firing initially induced by an unpredicted  
176 reward. By contrast, Figure 4 B (middle left panel) shows an early reward delivered after the  
177 half-way-mark (at the 300<sup>th</sup> time step), which induces lesser firing in VTA DA cells. The model  
178 is consistent with physiological data in primates, where earlier-than-expected rewards evokes  
179 progressively less firing as the reward delivery time increases (*Fiorillo et al., 2008*). Our model  
180 provides a mechanistic explanation for this data.

### 181 2. Variability in Magnitude

182 VTA Dopamine firing reflects the difference between the actual reward and the expected  
183 reward. For instance, VTA Dopamine neurons fire on US arrival if a reward is larger than  
184 expected (Figure 5 C middle panel). This corresponds to a positive reward prediction error,  
185 in accordance with physiological data. The subtractive nature of inhibition (*Eshel et al.,*  
186 *2015*) encodes the difference of magnitude between the actual magnitude of reward and the  
187 expected magnitude of reward (Figure 5C middle panel).

## 188 **Dissociation of time and magnitude prediction errors following VS Lesions**

### 189 1. VS lesion affects time prediction error

190 When an experimental lesion is made in the VS from rats (*Takahashi et al., 2016*), earlier-than-  
191 expected US does not trigger firing in VTA Dopamine cells. Accordingly, our model reproduces  
192 this lack of timing prediction error, as the virtual lesion of the VS in the model abolishes the  
193 VTA Dopamine response to earlier-than-expected US. Moreover, VTA GABA cells, instead of  
194 displaying a ramping signal, provide a constant tonic inhibition, similar to PPN FT, throughout  
195 the duration of the trial (Figure 5 A middle right panel). Indeed, the model posits that lack  
196 of dopamine firing for the VS-lesioned scenario compared to the control scenario is due  
197 to the higher inhibition from the VTA GABA neurons (Figure 5 A middle right panel). The  
198 VS inhibitory signal acts as a "when" signal providing VTA GABA neurons with information  
199 enabling computation of reward expectation at a given point in time. Due to this information  
200 being lost because of lesion, VTA GABA neurons do not have a ramping signal that peaks at  
201 the right moment. Instead, they have a constant inhibition throughout the interval.

202 2. VS lesion does not alter magnitude prediction error  
 203 The rewards with higher magnitude induce firing in VTA DA cells even if the VS is lesioned. A  
 204 reward that is double the magnitude triggers the same effect on US VTA Dopamine as in the  
 205 control scenario (Figure 5 B middle left panel).  
 206 Since the VS encodes only temporal information, its lesion does not affect the magnitude  
 207 encoding of the stimuli. This results in VTA DA firing showing the same subtractive effect as in  
 208 the control scenario(Figure 5 B middle left panel). This is due to the VTA GABA encoding the  
 209 magnitude from the BLA through the PPN FT neurons. A lack of VTA GABA ramping does not  
 210 prevent the VTA DA from having the magnitude encoded within its population, and provides  
 211 the same RPE at usual reward time. This behavior of VTA DA neurons in the case of a VS lesion  
 212 with larger magnitude is also in accordance with experimental results (*Takahashi et al., 2016*).

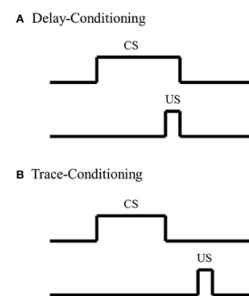


**Figure 2.** Delay Conditioning - In this paradigm, the conditioned stimulus (CS) persists until the presentation of the unconditioned stimulus (US)

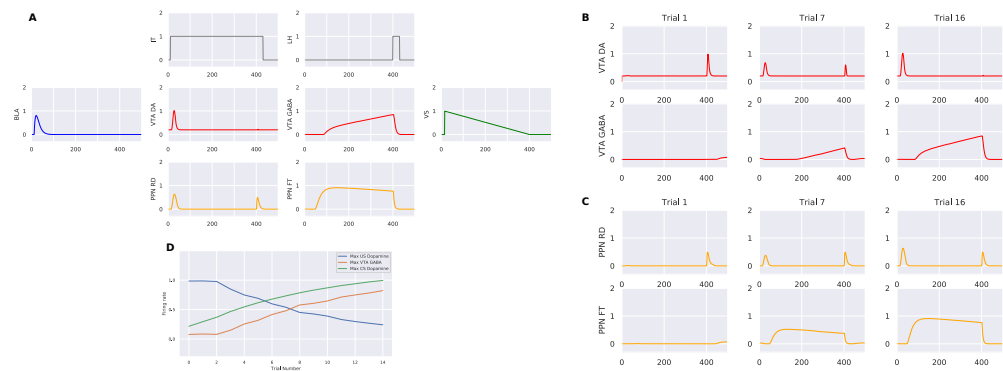


**Figure 3.** (A) The figure represents the firing of the neuronal populations after training following the same color conventions as the model architecture diagram. IT and LH indicate the stimulus and the reward respectively. PPN RD represent the phasic signals received from BLA and the LH at stimulus onset and reward delivery. VTA DA neurons show firing only at the arrival of the CS and VTA GABA neurons have a ramping expectation signal that fully cancels the VTA DA signal at reward delivery. BLA and VS have encoded magnitude and timing of the reward respectively. (B) This figure portrays the evolution of the VTA and PPN sub-populations throughout the duration of trials. VTA DA shows firing only at the reward delivery during initial trials while VTA GABA shows no firing due to absence of any expectation at this stage. At Trial 7, VTA DA shows twin peaks reflecting both a partial encoding at stimulus arrival and partial cancellation of reward signal. VTA GABA on the other hand has a ramping nature at the precise time of the arrival of the reward indicating encoding of timing and partial encoding of expectation. The final trial diagram shows the complete cancellation of the VTA DA signal at reward delivery and a complete encoding of stimulus at the CS arrival. Correspondingly, VTA GABA has a larger expectation signal that ramps that has completely encoded the magnitude of the reward signal. (C) shows the evolution of the PPN sub-populations during the sequence of trials with PPN RD signalling reward delivery from LH to VTA DA during the initial trials and PPN FT not showing any sign of expectation at the same time. In the middle of training, PPN RD reflects a partial firing for stimulus onset and the same reward signal firing as during the initial trials. PPN FT also reflects this partial firing with a tonic nature of firing that passes onto VTA GABA. During the final trial stages, PPN RD firing peaks for its stimulus arrival firing while a bigger tonic firing signal is observed for PPN FT. (D) portrays the evolution of VTA DA CS and US signals and that of VTA GABA. Both VTA GABA and VTA DA CS show increased firing across the trials while VTA DA US progressively reduces ultimately to the background firing rate of VTA DA. All the figures are averaged for 10 runs.

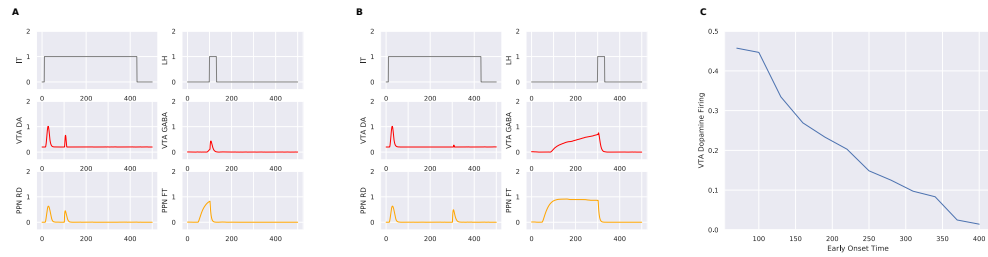


**Figure 4.** These figures indicate the early firing scenarios on VTA and PPN sub-populations. LH indicates the reward delivered earlier than usual and IT the stimulus. (A) denotes the arrival of the reward at 100<sup>th</sup> time step after training where VTA DA shows some firing compared to no firing after training when reward is delivered at the usual time. (B) This firing for an earlier reward is still larger than a later arrival of early reward at 300 time steps where VTA DA barely shows any firing. (C) indicates the progressively later "early" rewards fire less as early reward delivery times get closer to usual reward arrival times in accordance with data on (Fiorillo et al., 2008)

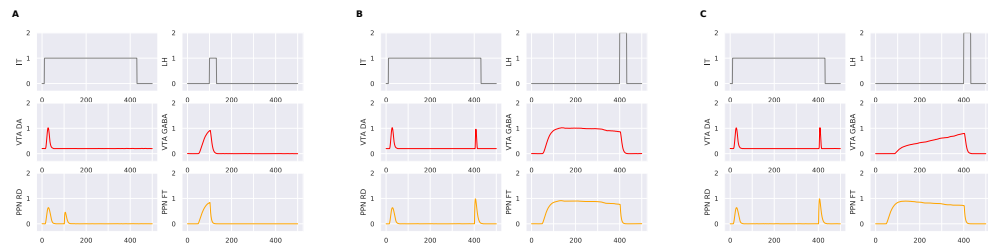


**Figure 5.** Panel 3- These figures indicate how timing information is lost but magnitude information of the reward is maintained on VTA sub-populations. LH indicates the reward delivered earlier than usual and IT the stimulus. During the VS lesion scenario, VTA GABA is no longer able to integrate the timing information coming from VS and just reflects the projection from PPN FT neurons. Hence, early rewards are treated as any other reward that comes at the usual time, reflecting no firing (left panel). But when the reward is of a higher magnitude (middle panel), it is able to indicate the prediction error just as in the control scenario where VS is not lesioned and VTA GABA integrates both magnitude and timing.

## 213 Discussion

### 214 Role of Timing in conditioning

215 The importance of CS-US interval timing is one of the key postulates of the proposed theory  
 216 underlying the model. In this model, the interval timing mechanism uses the dopamine signal  
 217 since the onset of the CS to learn the underlying temporal distribution to predict the arrival of the  
 218 reward, however it needn't be the case. Learning the interval time separating the CS and the reward  
 219 could happen without dopamine with a phenomenon called sensory-preconditioning (Sadacca  
 220 et al., 2016). Our model predicts that since time and magnitude are separate signals in the brain,  
 221 the learning of time precedes the learning of magnitude for reward prediction error to take place.  
 222 Interval timing learning in animals has been observed to happen in very few trials and sometimes  
 223 even one. The model posits that interval timing learning is an integral part of reward prediction  
 224 error computation in appetitive learning and the learning of timing happens before the magnitude  
 225 of the stimulus so as to construct an inhibitory signal that has a ramping nature before it ramps to  
 226 its maximum amplitude. The timing mechanism used in the model is very simplistic, reflecting the  
 227 learning of a single parameter to get the final slope of inhibition. It is possible that more complex  
 228 timing mechanisms are incorporated in the striatum to accommodate stochasticity in the temporal  
 229 interval.

230 This is consistent with the original Temporal Difference Reinforcement Learning (TDRL) represen-  
 231 tation of dopamine where the cue is tracked since the onset of its presentation, state by state until  
 232 reward is delivered as in the complete serial compound (CSC) stimulus representation (Schultz et al.,  
 233 1997). Here too, the state is tracked at each time point using the timing signal. However, unlike the  
 234 TD model, which is model-free and tracks value across states, this model learns a separate value  
 235 signal for state similar to the Successor Representation (SR)(Dayan, 1993) where reward and state

236 representation are computed separately unlike TD-Learning. This dissociation enables the model  
237 to learn changes in magnitude independent of the state and learn the state independent of the  
238 magnitude.

### 239 **Dual pathway model**

240 The dual pathway models of classical conditioning posit that the mechanism with which the CS firing  
241 occurs at the onset of a trained cue is dissociated from the expectation that inhibits the reward  
242 signal at the time of the reward. Our model too, largely follows the same pattern but with some  
243 deviations (*O'reilly et al., 2007*). This model replicates the observation in *Fiorillo et al. (2008)* about  
244 early rewards delivered at different time points exhibiting different firing. The interpretation of  
245 this model is that, this dopamine error is indicating a mismatch in state rather than a mismatch in  
246 magnitude. Since magnitude is a separate signal and does not require updating, the early reward  
247 firing is indicative of a violation of a belief of the state the animal is in. This prediction error is  
248 predicted to happen between the striatal inhibition and VTA GABA. This inhibition is also predicted  
249 to play a role in the lesion experiments done by *Takahashi et al. (2016)* where VS lesions hamper  
250 the ability of the animal in tracking state. This lesion in turn has an effect on VTA GABA which is no  
251 longer inhibited and only serves the magnitude component of the reward prediction error. Hence,  
252 early reward prediction errors no longer happen, because the animal does not recognize state  
253 prediction errors and expects the reward to happen all the time. It was also found in the study that  
254 VTA non dopamine neurons have a higher firing after the VS lesions consistent with our model and  
255 our model predicts, VTA GABA to have higher firing when VS is lesioned. This model hypothesis a  
256 continuous ramping signal that is active throughout the duration of the CS and the US, peaking at  
257 the time of the US and speculates that this inhibition signal and the CS firing could have the same  
258 source.

### 259 **Heterogeneity of PPN**

260 Though much of PPN's anatomical and chemical characteristics are unknown, studies have shown  
261 functional differences between populations inside PPN. Specific populations within PPN exist which  
262 fire phasically for rewards and others which have sustained firing from reward prediction to delivery  
263 of reward, and the activation sustaining till the delivery of the reward even if the arrival of the  
264 reward is delayed (*Okada and Kobayashi, 2009*). Moreover these neurons seem to encode amount  
265 of reward firing higher for rewards with larger magnitude (*Okada and Kobayashi, 2009*) (*Hong  
266 and Hikosaka, 2014*) portraying a graded firing signal capable of differentiating reward amounts  
267 consistent with this models characteristics. Studies have also pointed out a growing role for PPN  
268 projections to VTA non-dopamine neurons as necessary for appetitive pavlovian conditioning (*Yau  
269 et al., 2016*) and activation of PPN glutamate neurons to be reinforcing (*Yoo et al., 2017*). The  
270 hypothesis of this model is that a subset of PPN neurons (PPN FT) convey reward magnitude  
271 information to the VTA GABA neurons and any optogenetic silencing of these neurons can interfere  
272 with the computation of reward prediction error, though isolating these neurons could prove  
273 difficult owing the structures heterogeneity.

### 274 **VTA GABA theory of computing RPE in classical conditioning**

275 Previous studies have implicated the striatum (*Usuda et al., 1998*) as the source of the inhibitory  
276 signal cancelling the dopamine. But, recent projection-specific activation by optogenetic studies  
277 among others have shown that the inhibition from striatum has weak to no inhibitory effects on  
278 DA neurons when stimulating direct striatal inputs on DA neurons in the VTA (*Keiflin and Janak,  
279 2015*) (*Bocklisch et al., 2013*) (*Chuhma et al., 2011*) (*Xia et al., 2011*) (*Klein-Flügge et al., 2011*). There  
280 have been a number of recent results, suggesting an alternate pathway within VTA which might  
281 be responsible for this inhibitory signal. Moreover, optogenetic studies done on VTA (*Cohen et al.,  
282 2012*) (*Eshel et al., 2016*) have pointed out not only does the VTA GABA neurons exert enough  
283 inhibition to cancel VTA DA neurons but the inhibition is also subtractive in nature and hence



284 suitable for computation of reward prediction error (*Eshel et al., 2015*). This model hypothesises  
285 that the ramping nature of expectation which encodes both magnitude of the stimulus and time of  
286 arrival is encoded in the VTA GABA which acts as the site of integration between these two different  
287 dimensions of the reward. One possible explanation of this distributed nature of reward prediction  
288 error could be that this is what allows for rapid recomputation of values (either of time or magnitude)  
289 and allows the animal to exhibit and sometimes fast, adaptive behavior. Parallels could be drawn  
290 with the literature of reinforcement learning that the animals are not purely engaged in model-free  
291 reinforcement learning and that the dopamine signal itself could be not just performing reward  
292 prediction errors and differences in timing could elicit an error from the dopamine system for state  
293 prediction errors. For example, dopamine firing for early reward delivery could be interpreted as  
294 a state prediction error where the animals has to reevaluate the time of the reward rather than  
295 the magnitude of the reward. The precise interpretation of the dopamine prediction error could  
296 be handled by the upstream areas to determine what computations are to be done to reflect a  
297 changed scenario.

298 This model examines the role of VTA GABA in computing the reward prediction error along with  
299 a few other substrates based on some of the results provided by *Takahashi et al. (2016)*. This paper  
300 adopts a semi-markov approach to explain the findings while the model given here attempts to  
301 provide a system level model of how the underlying neuronal substrates might act. There are a few  
302 other behaviors that is observed in the model. The authors note that removing VS does not remove  
303 expectation and the animal in effect expects reward all the time, this could be the VTA GABA signal  
304 we observe in the model when VS is lesioned. VTA GABA loses its ramping functionality and has a  
305 flat tonic firing pattern carrying on its earlier peak expectation throughout the duration of the trial,  
306 The authors also note that "non-dopaminergic" neurons show significantly higher baseline firing  
307 rate when VS is lesion. Our model hypothesises that it is indeed the VTA GABA neurons that are  
308 now exhibiting a higher flat expectation due to the VS being lesioned. Thus, the model proposes  
309 that it is the VS input to VTA GABA that gives its expectation signal the temporal specificity that the  
310 authors mention in their paper.

## 311 **Methods and Materials**

### 312 **Evaluation of the model**

313 The paradigm used to evaluate the model is a simple CS-US associative learning task and also  
314 considers how the expectation cancels out the dopamine peak at the time of the reward. The trial  
315 duration is 500 time steps with each time step corresponding to 1ms. The stimulus is presented  
316 at the 10<sup>th</sup> time step and is kept switched on till the arrival of the reward at the 400<sup>th</sup> time step  
317 (400ms). The reward and the stimulus have by default a magnitude of 1. The number of trials for  
318 the entire conditioning to happen was set at 14 trials (i.e. trials required for the learning algorithm  
319 to converge).

### 320 **Model Description**

#### 321 **Computational principles**

322 The system-level model is composed of mean-field description of neuronal populations representing  
323 distinct, interconnected brain structures. Population dynamics is described by its average firing  
324 frequency across time  $U(t)$ , which is taken as the positive part of a membrane potential  $V(t)$ ,  
325 represented by the following equations:

$$326 \tau \cdot \frac{dV(t)}{dt} = (-V(t) + g_{exc}(t) - g_{inh}(t) + B + \eta(t)) \quad (2)$$

$$327 U(t) = (V(t))^+ \quad (3)$$

326 Here  $\tau$  is the time constant of the cell,  $B$  is the baseline firing rate and  $\eta(t)$  is the additive noise  
 327 term chosen randomly at each time step from a uniform distribution between  $-0.01$  and  $0.01$ .  
 328 The incoming afferent synaptic currents  $g_{exc}$  and  $g_{inh}$  represent the weighted sum of excitatory  
 329 and inhibitory firing rates, respectively, the weight representing the synaptic weights between the  
 330 populations.

331 Some of the neuronal populations extract a short-term phasic activity from their incoming  
 332 inputs, by removing out the tonic component of the input. This is done by the following equations:

$$\tau \cdot \frac{d\bar{x}(t)}{dt} = (-\bar{x}(t) + x(t)) \quad (4)$$

$$\phi_{\tau,k}(x(t)) = (x(t) - k \cdot \bar{x}(t))^+ \quad (5)$$

333 Here  $\bar{x}(t)$  integrates the incoming input  $x(t)$  with a time constant  $\tau$  and thus represents the tonic  
 334 component of the input, while  $\phi_{\tau,k}(x(t))$  represents the positive part of the difference between  
 335  $x(t)$  and  $\bar{x}(t)$ . Hence, The constant  $k$  controls how much of the original input is kept, a  $k$  value  
 336 of 0 indicates the entire synaptic input is to be preserved and a  $k$  value of 1 outputs the phasic  
 337 component only, i.e. the entire tonic component has been entirely removed.

A Bound function is used when the firing of a population is described with an upper and a lower  
 limit in certain populations.

$$\psi(x) = \begin{cases} 0 & \text{if } x < 0 \\ x & \text{if } 0 < x < 1 \\ 1 & \text{if } x > 1 \end{cases} \quad (6)$$

338 A threshold function is also used in some populations and it outputs 1 when the input exceeds  
 339 a threshold  $\Gamma$ , 0 otherwise:

$$\Delta_{\Gamma}(x) = \begin{cases} 0 & \text{if } x < \Gamma \\ 1 & \text{otherwise} \end{cases} \quad (7)$$

The learning rules defined in the model are based on the Hebbian learning rule and a DA  
 modulated learning rule in the case of BLA like the multiplicative three factor learning rule. The  
 evolution over time of the weight  $w(t)$  of a synapse between the neuronal population *pre* (presynaptic  
 neurons) and the neuronal population *post* (postsynaptic neurons) is governed by:

$$\frac{dw(t)}{dt} = (\alpha \cdot U_{pre}(t) \cdot U_{post}(t)) \quad (8)$$

340 where  $w$  is the weight term,  $\alpha$  the learning rate,  $U_{pre}(t)$  and  $U_{post}(t)$  are indicating the firing rates of  
 341 the presynaptic and postsynaptic neuronal populations, respectively.

## 342 Population definitions

### 343 Representations of inputs

344 The sensory inputs of the CS and the reward input of the US are encoded by the inferotemporal  
 345 cortex (IT) and the lateral hypothalamus (LH), respectively, simply as square wave signals:

$$U(t) = I(t)^+ \quad (9)$$

346 where  $I(t)$  is an external input resulting either from a stimulus or from a reward.

### 347 Basolateral Amygdala

348 The BLA receives inputs about the CS from the IT, the US from the LH, as well as VTA DA output. This  
349 allows the BLA to learn to associate the CS with the US, thus providing a magnitude expectation.  
350 The equation below is the same equation as in Equation 2 without the inhibitory component and  
351 with the presence of a tonic to phasic conversion.

$$\tau \cdot \frac{dV(t)}{dt} = (-V(t) + \phi_{\tau_{exc},k}(g_{exc}(t)) + \eta(t)) \quad (10)$$

$$U(t) = (V(t))^+$$

with  $\tau = 10\text{ms}$ ,  $\tau_{exc} = 10\text{ms}$ ,  $k = 1$ .

The CS is learned by updating the synaptic weights between IT and BLA and the learning rule is given by:

$$\frac{dw(t)}{dt} = D \cdot \alpha \cdot U_{pre}(t) \cdot (U_{mag} - U_{post}(t))^+ \quad (11)$$

352 Here  $D$  indicates the presence of the US corresponding to the dopaminergic neuronal modulation  
353 from the VTA,  $\alpha$  is the learning rate equal to 0.003,  $U_{mag}$  is the magnitude of LH firing,  $U_{pre}$  and  $U_{post}$   
354 are the firing rates of presynaptic and postsynaptic neurons, respectively.

### 355 Central Amygdala

356 The CE is the output nuclei of the amygdala and it projects to both the PPN nuclei, relaying  
357 information from the BLA. The CE projects to the PPN RD neurons that convey US and CS firing to  
358 the VTA dopamine neurons and PPN FT neurons that convey reward expectation.

359 The equations for the membrane potential and the firing rate are the same as Equation 10 and  
360 Equation 3, respectively, with  $\tau = 20\text{ms}$ ,  $\tau_{exc} = 5\text{ms}$ ,  $k = 1$ .

361

### 362 Pedunclopontine nucleus

363 The PPN has two distinct populations in this model for reward and expectation. The PPN is a  
364 heterogeneous structure both in terms of neuronal populations and of responses during classical  
365 conditioning (*Okada and Kobayashi, 2009*). Hence, we modeled two distinct subpopulations reflect-  
366 ing the two major classes of responses found experimentally: FT (Fixation Target) population, which  
367 activates briefly upon CS or US presentation, and RD (Reward Delivery) population, which display  
368 sustained activity during the CS-US interval.

### 369 PPN RD

370 The PPN Reward Delivery neurons signal the occurrence of the CS and the US from the CE and the  
371 LH, respectively. It also contains a sub-population of inhibitory neurons that inhibits the PPN FT  
372 neurons.

373 The equations for the membrane potential and the firing rate are the same as Equation 10 and  
374 Equation 3 respectively, with  $\tau = 5\text{ms}$ ,  $\tau_{exc} = 5\text{ms}$ ,  $k = 1$ .

375

### 376 PPN FT

377 The PPN FT neurons encode the magnitude expectation delivered to the VTA GABA neurons. The  
378 PPN FT neurons receive information from the CE and are inhibited by the PPN RD neurons. They  
379 serve to maintain a constant magnitude that is conveyed to the VTA GABA neurons for final reward  
380 prediction error computation. The equations for the membrane potential and the firing rate are  
381 the same as Equation 2 without baseline firing and Equation 3 respectively with  $\tau = 5\text{ms}$ .

382

### 383 Ventral Striatum and OFC

384 It has long been thought that the Ventral Striatum (VS) is responsible for the reward prediction term  
 385 in RPE calculation. In our model, the VS encodes the duration of the CS-US interval only. The VS is  
 386 composed of inhibitory cells, and signals the timing of expected reward to VTA GABA cells through  
 387 a decrease in activity. The OFC (Orbitofrontal Cortex) relays the presence of the US from the IT  
 388 to the VS. Then, a simplified timing model comprising a negative integrator similar to the timing  
 389 algorithm in *Rivest and Bengio (2011)* signals the interval duration through a slowly decreasing  
 390 activity until the expected timing of the US. To do so, the integrator here has an amplitude of 1 at  
 391 the beginning of the trial and after weight updating, decreases its firing to 0 at the precise time of  
 392 reward delivery. In this framework, learning the CS-US interval consists in adjusting the slope of the  
 393 slowly-decreasing activity.

### 394 Mechanism of timing

395 The timing mechanism in the VS transforms a phasic excitatory input into a decreasing sustained  
 396 activity, which slope depends upon the weights.

$$\tau \cdot \frac{dV(t)}{dt} = (g_{exc}(t)) - V \cdot \Delta_{\Gamma}(\phi_{\tau_{mod},k}(g_{mod}(t)) - \bar{B}) + \eta(t) \quad (12)$$

$$U(t) = (g_{exc}(t) - \Delta_{\Gamma}(\phi_{\tau_{mod},k}(g_{mod}(t)) - \bar{B}) - \psi(V(t)))^+ \quad (13)$$

397 with  $\tau = 1\text{ms}$ ,  $\tau_{mod} = 5\text{ms}$ ,  $k = 1$ ,  $\Gamma = 6$  and  $\bar{B}$  is the baseline firing rate from VTA dopamine to  
 398 VS.  $\Gamma$  ensures a minimum threshold to be achieved for the VTA dopamine phasic firing to enable  
 399 modulation.  $\psi()$  is a bounded function.

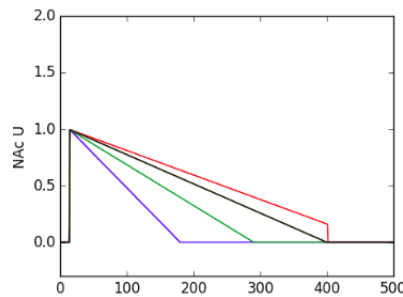


**Figure 6.** The slope is decreased at every iteration until it exceeds the duration (the red line) enabling exact correction of the weight encoding the duration to be found (the black line). The colors indicate the progressive iterations

As described in figure 6, weight is updated after each iteration according to the following rule:

$$\frac{dw(t)}{dt} = (-\alpha \cdot w + \Delta_{\Gamma}(U(t)) \cdot w \cdot (U(t)/(1 - U(t)))) \quad (14)$$

400 where  $\alpha$  is the learning rate equal to 0.4 The first term decreases the weights based on  $\alpha$  and  
 401 the weights keep decreasing until the bound is reached when  $\Delta_{\Gamma}(U(t))$  becomes greater than 0 at  
 402 the time of the reward. The correcting update is the second term of the weight updating and the  
 403 slope is increased with a weight increase encoding the duration of the interval.

404

405 It should be noted that the model postulates that the learning of time happens before the  
 406 learning of value of the stimulus, i.e., its magnitude.

407 VTA

408 The VTA comprises two major neuronal populations, dopaminergic (DA) and gabaergic (GABA),  
409 glutamatergic cells representing less than 3 percent of VTA cells. VTA GABA neurons locally inhibit  
410 VTA DA neurons and participate in the computation of reward prediction error in VTA DA cells (**Cohen**  
411 **et al., 2012**). More precisely, VTA GABA neurons display a sustained, slowly-increasing ramping  
412 activity during the CS-US interval (**Eshel et al., 2015**) but only significantly affect phasic DA activity  
413 (i.e. the RPE) rather than tonic DA activity during the interval. We thus modeled the two populations  
414 from the VTA as follows.

415 VTA Dopamine

416 The VTA dopaminergic (DA) neurons receive excitatory inputs from the PPN RD population, which  
417 conveys actual reward and reward prediction from the amygdala; and inhibitory inputs from the  
418 VTA GABA cells, which signal reward expectation. The difference between these excitatory and  
419 inhibitory inputs constitutes the reward prediction error (RPE) (**Sutton and Barto, 1998**) (**Glimcher,**  
420 **2011**). VTA DA neurons broadcast this RPE to the system. During learning, VTA DA neurons initially  
421 fire upon US reward delivery. This US activity progressively gets canceled by VTA GABA signaling the  
422 reward expectation, and at the same time, phasic firing upon CS arrival develops with learning.

$$\tau \cdot \frac{dV(t)}{dt} = (-V(t) + \phi_{\tau exc, k}(g_{exc}(t)) - \phi_{\tau inh, k}(g_{inh}(t)) + \eta(t))$$

$$U(t) = (V(t) + B)^+ \quad (15)$$

423 With  $\tau = 5ms$ ,  $\tau_{exc} = 5ms$ ,  $k = 1$  and  $B$  is the baseline firing rate of the VTA Dopamine equal to 0.2  
424

425 VTA GABA

426 VTA GABA neurons combine inputs from the VS, which encodes the expected time of reward, and  
427 from the PPN, which signals expected reward magnitude. VTA GABA neurons thus encode reward  
428 expectation and inhibit VTA DA neurons. The equation for membrane potential is the same as in  
429 Equation 2 without baseline firing and population dynamics follows Equation 3 with  $\tau = 20ms$ .

430 This model is implemented in Python, and uses the DANA library for neuronal computation  
431 (**Rougier and Fix, 2012**). Description of all the other model parameters is detailed in Table 1. The  
432 model can be accessed in the following link : [https://github.com/palladiun/Pavlovian-Conditioning-](https://github.com/palladiun/Pavlovian-Conditioning-VTA-GABA)  
433 VTA-GABA

Architectural parameters		
Parameter	Meaning	Value
US input_size	size of input vectors from LH	1
CS input_size	size of input vectors from IT	4
VTA Dopamine_size	number of neurons in VTA Dopamine	10
VTA GABA_size	number of neurons in VTA GABA	5
BLA_size	number of neurons in BLA	1
CE_size	number of neurons in CE	1
OFC_size	number of neurons in OFC	1
PPN RD_size	number of neurons in PPN RD	4
PPN FT_size	number of neurons in PPN FT	4
PPN Magnitude_size	number of neurons in PPN Magnitude	4
Equation parameters		
BLA_CE	constant weights from BLA to CE	0.15
LH_PPN_RD	constant weights from LH to PPN_RD	1.2
LH_BLA	constant weights from LH to BLA	1
IT_OFC	constant weights from IT to OFC	.25
CE_PPN_RD	constant weights from CE to PPN_RD	2
CE_PPN_Mag	constant weights from CE to PPN_Mag	.3
PPN_RD_PPN_Mag	constant weights from PPN_RD to PPN_Mag	0.8
PPN_RD_VTA_Dop	constant weights from PPN_RD to VTA_Dop	1
PPN_Mag_PPN_Rel	constant weights from PPN_Mag to PPN_Rel	0.2
VS_PPN_Rel	constant weights from VS to PPN_Rel	1
PPN_Rel_VTA_GABA	constant weights from PPN_Rel to VTA_GABA	0.25
VTA_Dopamine_BLA	constant weights from VTA_Dopamine to BLA	1
VTA_Dopamine_VS	constant weights from VTA_Dopamine to VS	1
VTA_GABA_VTA_Dopamine	constant weights between VTA_GABA and VTA_Dopamine	0.2
OFC_VS	initial weights between OFC and VS	0.006
IT_BLA	initial weights between OFC and VS	0.01

**Table 1.** Table describing network architecture and parameters used in activation and learning rules.

## 434 Acknowledgments

435 We would like to acknowledge the following grants which have been a major support to this  
436 research.

- 437 • Indo-French CEFIPRA Grant for the project Basal Ganglia at Large (No. DST-INRIA 2013-02/Basal  
438 Ganglia dated 13-09-2014)
- 439 • Internships programme at INRIA, 6 month Internship with Team Mnemosyne at INRIA Bor-  
440 deaux - Sud-Ouest

441 We also thank Maxime Carrere for helpful discussions.

## 442 References

- 443 **Bocklisch C**, Pascoli V, Wong JC, House DR, Yvon C, De Roo M, Tan KR, Lüscher C. Cocaine disinhibits dopamine  
444 neurons by potentiation of GABA transmission in the ventral tegmental area. *Science*. 2013; 341(6153):1521–  
445 1525.
- 446 **Carmichael S**, Price JL. Sensory and premotor connections of the orbital and medial prefrontal cortex of  
447 macaque monkeys. *Journal of Comparative Neurology*. 1995; 363(4):642–664.
- 448 **Chuhma N**, Tanaka KF, Hen R, Rayport S. Functional connectome of the striatal medium spiny neuron. *Journal*  
449 *of Neuroscience*. 2011; 31(4):1183–1192.
- 450 **Cohen JY**, Haesler S, Vong L, Lowell BB, Uchida N. Neuron-type specific signals for reward and punishment in  
451 the ventral tegmental area. *nature*. 2012; 482(7383):85.
- 452 **Dayan P**. Improving generalization for temporal difference learning: The successor representation. *Neural*  
453 *Computation*. 1993; 5(4):613–624.
- 454 **Eshel N**, Bukwich M, Rao V, Hemmelder V, Tian J, Uchida N. Arithmetic and local circuitry underlying dopamine  
455 prediction errors. *Nature*. 2015; 525(7568):243.
- 456 **Eshel N**, Tian J, Bukwich M, Uchida N. Dopamine neurons share common response function for reward  
457 prediction error. *Nature neuroscience*. 2016; 19(3):479.
- 458 **Fiorillo CD**, Newsome WT, Schultz W. The temporal precision of reward prediction in dopamine neurons. *Nature*  
459 *neuroscience*. 2008; 11(8):966–973.
- 460 **Fiorillo CD**, Tobler PN, Schultz W. Discrete coding of reward probability and uncertainty by dopamine neurons.  
461 *Science*. 2003; 299(5614):1898–1902.
- 462 **Fiorillo CD**, Tobler PN, Schultz W. Evidence that the delay-period activity of dopamine neurons corresponds to  
463 reward uncertainty rather than backpropagating TD errors. *Behavioral and brain Functions*. 2005; 1(1):7.
- 464 **Glimcher PW**. Understanding dopamine and reinforcement learning: the dopamine reward prediction error  
465 hypothesis. *Proceedings of the National Academy of Sciences*. 2011; 108(Supplement 3):15647–15654.
- 466 **Hollerman JR**, Schultz W. Dopamine neurons report an error in the temporal prediction of reward during  
467 learning. *Nature neuroscience*. 1998; 1(4):304.
- 468 **Hong S**, Hikosaka O. Pedunculopontine tegmental nucleus neurons provide reward, sensorimotor, and alerting  
469 signals to midbrain dopamine neurons. *Neuroscience*. 2014; 282:139–155.
- 470 **Janak PH**, Tye KM. From circuits to behaviour in the amygdala. *Nature*. 2015; 517(7534):284.
- 471 **Joel D**, Niv Y, Ruppin E. Actor–critic models of the basal ganglia: New anatomical and computational perspectives.  
472 *Neural networks*. 2002; 15(4-6):535–547.
- 473 **Keiflin R**, Janak PH. Dopamine prediction errors in reward learning and addiction: from theory to neural circuitry.  
474 *Neuron*. 2015; 88(2):247–263.
- 475 **Klein-Flügge MC**, Hunt LT, Bach DR, Dolan RJ, Behrens TE. Dissociable reward and timing signals in human  
476 midbrain and ventral striatum. *Neuron*. 2011; 72(4):654–664.
- 477 **Kobayashi Y**, Okada KI. Reward prediction error computation in the pedunculopontine tegmental nucleus  
478 neurons. *Annals of the New York Academy of Sciences*. 2007; 1104(1):310–323.

- 479 **Lokwan S**, Overton P, Berry M, Clark D. Stimulation of the pedunclopontine tegmental nucleus in the rat  
480 produces burst firing in A9 dopaminergic neurons. *Neuroscience*. 1999; 92(1):245–254.
- 481 **Niv Y**, Duff MO, Dayan P. Dopamine, uncertainty and TD learning. *Behavioral and brain Functions*. 2005; 1(1):6.
- 482 **Okada KI**, Kobayashi Y. Characterization of oculomotor and visual activities in the primate pedunclopontine  
483 tegmental nucleus during visually guided saccade tasks. *European Journal of Neuroscience*. 2009; 30(11):2211–  
484 2223.
- 485 **Okada Ki**, Kobayashi Y. Reward prediction-related increases and decreases in tonic neuronal activity of the  
486 pedunclopontine tegmental nucleus. *Frontiers in integrative neuroscience*. 2013; 7.
- 487 **O'reilly RC**, Frank MJ, Hazy TE, Watz B. PVLV: the primary value and learned value Pavlovian learning algorithm.  
488 *Behavioral neuroscience*. 2007; 121(1):31.
- 489 **Pan WX**, Schmidt R, Wickens JR, Hyland BI. Dopamine cells respond to predicted events during classical  
490 conditioning: evidence for eligibility traces in the reward-learning network. *Journal of Neuroscience*. 2005;  
491 25(26):6235–6242.
- 492 **Pavlov IP**. Conditional reflexes: An investigation of the physiological activity of the cerebral cortex. H. Milford;  
493 1927.
- 494 **Rivest F**, Bengio Y. Adaptive drift-diffusion process to learn time intervals. arXiv preprint arXiv:11032382. 2011; .
- 495 **Rougier NP**, Fix J. DANA: distributed numerical and adaptive modelling framework. *Network: Computation in*  
496 *Neural Systems*. 2012; 23(4):237–253.
- 497 **Sadacca BF**, Jones JL, Schoenbaum G. Midbrain dopamine neurons compute inferred and cached value  
498 prediction errors in a common framework. *Elife*. 2016; 5:e13665.
- 499 **Sah P**, Faber EL, De Armentia ML, Power J. The amygdaloid complex: anatomy and physiology. *Physiological*  
500 *reviews*. 2003; 83(3):803–834.
- 501 **Schultz W**, Dayan P, Montague PR. A neural substrate of prediction and reward. *Science*. 1997; 275(5306):1593–  
502 1599.
- 503 **Semba K**, Fibiger HC. Afferent connections of the laterodorsal and the pedunclopontine tegmental nuclei  
504 in the rat: a retro-and antero-grade transport and immunohistochemical study. *Journal of Comparative*  
505 *Neurology*. 1992; 323(3):387–410.
- 506 **Sutton RS**, Barto AG. Reinforcement learning: An introduction, vol. 1. MIT press Cambridge; 1998.
- 507 **Takahashi YK**, Langdon AJ, Niv Y, Schoenbaum G. Temporal specificity of reward prediction errors signaled by  
508 putative dopamine neurons in rat VTA depends on ventral striatum. *Neuron*. 2016; 91(1):182–193.
- 509 **Usuda I**, Tanaka K, Chiba T. Efferent projections of the nucleus accumbens in the rat with special reference to  
510 subdivision of the nucleus: biotinylated dextran amine study. *Brain research*. 1998; 797(1):73–93.
- 511 **Vitay J**, Hamker FH. Timing and expectation of reward: a neuro-computational model of the afferents to the  
512 ventral tegmental area. *Frontiers in neurorobotics*. 2014; 8.
- 513 **Xia Y**, Driscoll JR, Wilbrecht L, Margolis EB, Fields HL, Hjelmstad GO. Nucleus accumbens medium spiny  
514 neurons target non-dopaminergic neurons in the ventral tegmental area. *Journal of Neuroscience*. 2011;  
515 31(21):7811–7816.
- 516 **Yau HJ**, Wang DV, Tsou JH, Chuang YF, Chen BT, Deisseroth K, Ikemoto S, Bonci A. Pontomesencephalic tegmental  
517 afferents to VTA non-dopamine neurons are necessary for appetitive Pavlovian learning. *Cell reports*. 2016;  
518 16(10):2699–2710.
- 519 **Yoo JH**, Zell V, Wu J, Punta C, Ramajayam N, Shen X, Faget L, Lilascharoen V, Lim BK, Hnasko TS. Activation of  
520 pedunclopontine glutamate neurons is reinforcing. *Journal of Neuroscience*. 2017; 37(1):38–46.